CALCULATION OF THE DRAG OF A SHIP HULL USING RANS

Carlos José Rocha de Oliveira Castro
Escola Politécnica da USP – Dept. Naval Engineering
Carlos.jose@poli.usp.br

Fabio Saltara
Escola Politécnica da USP – Dept. Mechanical Engineering
fsaltara@usp.br

Abstract. *In this work it will be presented the methodology and the results of the three-dimensional computational simulation of the rectilinear displacement in constant speed, of the container carrier KRISO KCS. The simulation was carried out by the solution of the RANS equations for viscous incompressible flow, using the finite volumes method with an unstructured mesh. In the simulation the influence of the free surface was not considered. The influence of the turbulence in the viscous friction was analyzed, as well as the influence of the mesh refinement. The turbulence was modeled with the SST k-ω model with wall functions. The resulsts show reasonable agreement with experiments.*

Keywords*: RANS, turbulence, ship.*

1. Introduction

The main motivation for the use of numerical models to the study of the flow around a ship is the evaluation of the hydrodynamic resistance of the hull without the necessity of expensive and time-consuming model tests in towing tanks. Beyond this there is the question of the efficiency of the propulsion system. The effect of the wake of the hull on the performance of the propeller is well known qualitatively but there is a great difficulty in estimating it. Usually the task is done using experimental tests.The methods of CFD based on RANS (Reynolds Averaged Navier Stokes) equations have the potential to allow the analysis of details of the flow and the interaction between the hull, propeller and the appendices.

In this article it is described the first necessary stage for any global analysis of hydrodynamic aspects of a ship; the calculation of the resistance and the wake profile in the region of the rudder and propeller. Once we succeed in this first step we can move to more complex and particular aspects of the ship hydrodynamics.

For the verification of the numerical results it has been used the experimental values gotten by KRISO (Korea Research Institute of Ships and Ocean Engineering) for the model KCS, a 3600 containers carrier. This model has a characteristic bulb in the bow that reduces the wave making, and there is also another one in the stern. Nevertheless, the work was developed without taking into account the influence of the free surface and the effect of wave making, witch is discussed ahead. The figure.1 shows the three-dimensional model of the hull wetted surface. The simulation will be based on a geometric model with the same dimensions of the reduced model used in the tests to allow the direct comparison with the experimental values. It is a 7.27m length and 0.60m width model, towed at a speed of 2.196m/s, which means a Froude number of Fn=0.26 and a Reynolds number $Re=1.4x10^7$.

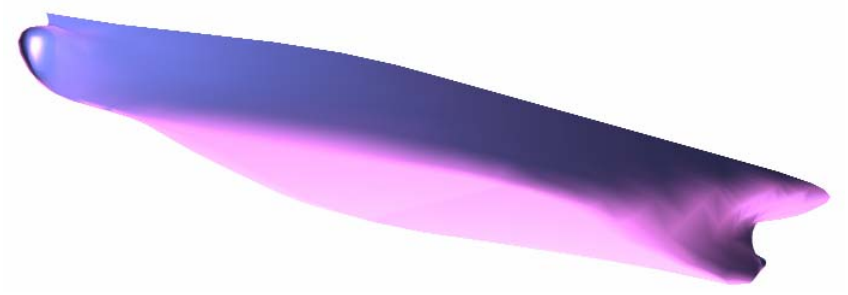

Figure 1. Geometric model of the ship's hull

2. Numerical Method

For the solution of the RANS it was used the commercial package Fluent, that is based on a finite volumes solver. The domain discretization is made using co-located meshes, based in an arrangement like the proposed by Rhie& Chow (1983) to prevent the oscillations of pressure and speed, typical of this type of meshes.

The calculation was made in stationary state, using linear interpolation for the pressure in the volume faces, a second order upwind scheme for the convective terms and the SIMPLEC algorithm for the pressure-velocity coupling. The equations system was solved using the standard Gauss-Siedel iterative method. In the initial phase of the project some combinations with other numerical models had been tested and were chosen the ones that presented better commitment between precision and speed.

The free surface was substituted by a symmetry plan, what reduces the precision of the global model once part of the hull resistance is related to the energy spend in the wave making, an effect that can not be taken into account with the symmetry plane. Because this parcel will not be considered we must be careful when comparing the numerical results with the experiments. Nevertheless this has been a common practice because it greatly simplifies the problem and other important information can be acquired without great loss of accuracy.

2.1. Turbulence Model

To determine the boundary layer profile it was used the SST k-ω turbulence model with wall functions of the Launder-Spalding type. The flow around the hull has strong three-dimensional effects, favorable and adverse pressure gradients, and regions of recirculation. Moreover the conditions of turbulence in the free flow are estimated, so it becomes desirable a model that does not have much sensitivity to the free stream conditions. The k-ω model in general performs better than the k-ε model when there are adverse pressure gradients. Nevertheless, the k-ω model is sensitive to the free-stream boundary conditions. More details can be found in Wilcox [21].

For this reasons the SST k-ω model looks to be the most adequate. In the SST model the k-ω equations are solved only inside the boundary layers and the standard k-ε model, with the dissipation equation written in terms of ω instead of ε, is used elsewhere. This double behavior guarantees accurate results inside the boundary layer and eliminates the problem of the free-stream sensitivity of the k-ω model. See further discussion in [3], [9] and [11].

The SST k-ω model was applied together with wall functions to avoid the high level of grid refinement close to the wall necessary to the direct integration in the viscous sublayer. Using wall functions instead of locating the first grid node at $y+<1$ we can use $y+\approx100$, inside the log-layer.

2.2. Mesh and Boundary Conditions

In complex three-dimensional geometries as it is the case of the hull of a ship the generation of a structured mesh is an extremely arduous task and demands much time of preparation.

With unstructured mesh generators the task is easier and faster. Nevertheless they do not admit a satisfactory level of control of the dimensions and growth of the mesh elements. Inside of a domain so extensive like that used to the calculation of the flow around a ship it is difficult to generate a fine mesh close to the wall, with some elements inside of the boundary layer, together with a coarse mesh in the free stream.

The figure.2 below shows the full domain and the tetrahedral mesh with two details.

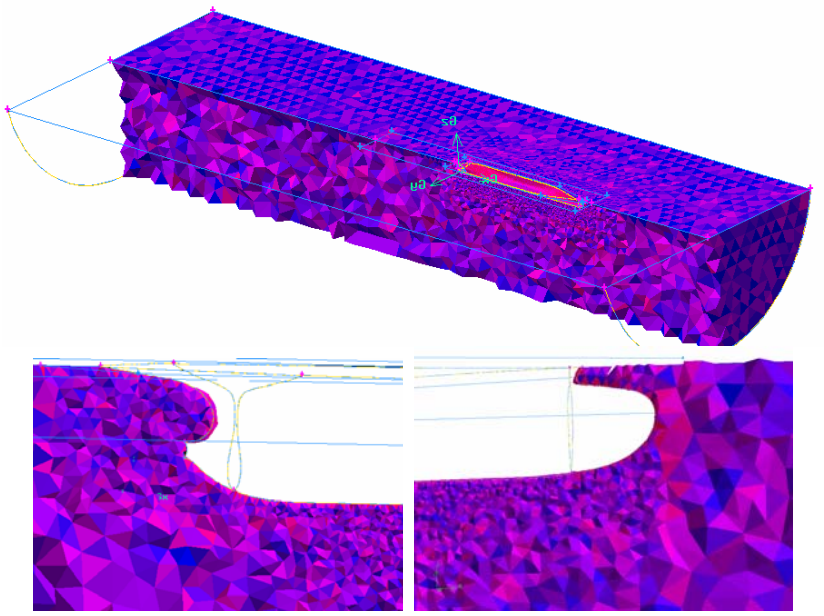

Figure 2. The upper figure shows the mesh across the computational domain, below at right a detail of the mesh in the stern region, and at the left at the stern region

The hull surface mesh used in this study is very refined, more than is usual in hull simulations. The cause of this is the trend of the tetrahedral mesh generator to create the elements with edges of same size. Therefore as the heights of the first elements have to be small, its lateral edges are very small too. The calculation domain was chosen based in the cases presented for Stern [20].

At the upstream of the hull it was adopted a velocity inlet plane with V=2.196 m/s normal to the surface (that is the velocity of the ship at the experiment), at the downstream it was used an outflow surface, at the upper side a symmetry plane and at the sides a cylindrical wall with zero shear stress that have the function of the channel wall. The hull surface was defined as a wall with non-slip condition

In order to validate the procedure, 3 meshes of different dimensions were used:

Table 1: Some details of the three meshes used

Grid	Δl_0	Growth factor	N° of volumes
II	10	1.15	1.651.725
III	15	1.15	1.110.207
IV	22.5	1.15	727.356

The mesh was generated automatically without local refinements, except in one case (the mesh I), and without regions of mesh overlapping. Although it had presented good homogeneity, the elements next to the most bended surfaces of the hull had a deficient skewness (aspect rate). Beyond these three cases (II, III and IV) a fourth was adopted based in the mesh (II), but with a local refinement in the region of the propeller and bow.

3. Numerical Results

First we carried out inviscid simulations to generate initial conditions to speed up the convergence of the turbulent calculations. At the end of each simulation it was made a test of the convergence criteria based on the residue. Initially the adopted criteria was a residual E=10-3. After we got the convergence for this residual, the result of the drag was calculated and the symmetry of the pressure and speed fields in the domain was checked graphically. After that the convergence residual was reduced of an order of magnitude, successively, until the total resistance did not have more significant alteration (<1%).

This check demonstrated that the adequate criterion of convergence is $E=5.10^{-6}$ in the conservation of mass for the inviscid calculation and $E=1.10^{-5}$ in the kinetic energy (k) for the turbulent flow. Also the total drag on the surface of the hull was monitored and this number supplied a good indication of how the solution was converging. The total drag stabilizes in a fixed value when the residue arrived at the final values previously described.

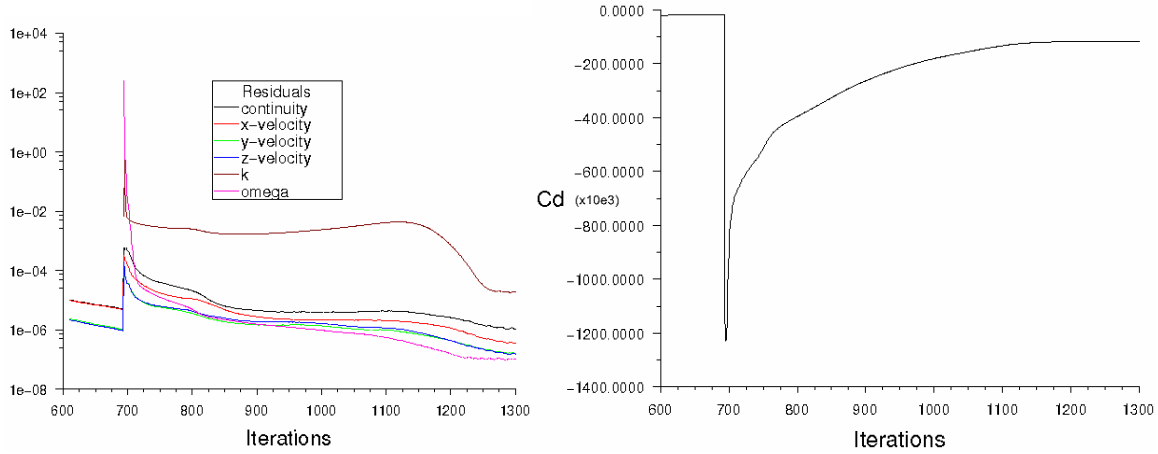

Figure 3: Convergence history of the variables residuals and the drag coefficient.

3.1. Comparison of force coefficients

The comparison was made with relation to the coefficient of total resistance (*Ct*). The total resistance of a hull can be divided into three distinct parts: a viscous parcel, a form parcel due to the pressure distribution and a wave making parcel. The adoption of a symmetry plane instead of a free surface is a great difference between the experiment and the

simulation that limits the direct comparison of the data because it does not take into account the wave making resistance parcel. For this type of ships, that has a relatively low Froude number, the parcel of resistance due the wave making represents the smaller fraction of the total resistance, however its value has the same error order of magnitude that is observed in the simulations, making difficult to make a direct comparison between the numerical model and the test.

Table 2: Numerical results with different meshes. Fv: viscous resistance; Fres: residual resistance; Ft: total resistance; Ft correct= Ft – wave resistance; all forces in Newtons;

Numerical evaluation				experiment			*Difference*		
Grid	Fv	Fform	Ft	Fv	Fres	Ft	**Fv**	Ft	Ft correct
I	62.66	9.88	72.54	65.1	15.84	80.94	**-3.75%**	**-10.38%**	**1.58%**
II	62.54	11.7	74.23	wave resistance (Fwave):	9.53		**-3.93%**	**-8.29%**	**3.95%**
III	60.94	12.57	73.51	form drag(Fform):	6.51		**-6.39%**	**-9.18%**	**2.94%**
IV	57.49	13.16	70.64				**-11.69%**	**-12.73%**	**-1.08%**

Three meshes were used to try to get the validation of the method and estimate its uncertainty. Case I mesh was generated from the II mesh with more refinement in the region of the bow and stern, to correct the awful skewness that the elements presented in those regions. The value of the *Ct* (total resistance coefficient) that was obtained experimentally is 0.00352, with an uncertainty of 6%. All the calculated values are below it, as is expected because in the experiments it is included the wave-making resistance. The difference between the experimental and calculated values are a little above of what has been obtained in some recent works. Most of them are in the 4% to 7% band.

It can also be seen in table 2 that the parcel of the viscous resistance is far more significant than that of form resistance (84% of the resistance in case II is due the viscous resistance). Therefore the use of models that obtain a better solution of the boundary layer speed profile and that can calculate with more precision the wall friction will improve the accuracy of the results. The recent works made by varied authors are predominantly based on low Re methods for the region of the boundary layer, and direct integration, in contrast of this work where wall functions were used. This is possibly the reason to the less accurate results in our calculations when compared with other authors that published recently.

The procedure used by KRISO to estimate the viscous resistance was the ITTC 1978 method [8]. According to this procedure the estimate is based on the friction over a plain plate with the same wetted surface of the hull. The viscous resistance parcel obtained is Fv=65.1N. Curiously the best result was not obtained with mesh I, the most refined and with correction of the elements shape in the region of the bow, but with the mesh II, which presented a viscous resistance Fv=62.54N. However both the results obtained with the meshes I and II are close to the one traditionally estimated. In the KRISO model tests the calculated residual resistance was F_{res}=15.84N.

The error is concentrated more in the estimate of the F_{res} (residual force) that groups the effect of the form drag and wave making resistance. The correct estimate of this parcel has been always a challenge. Usually it is made based on relations obtained from a series of reduced model tests with hulls of similar shapes. Another method is to use the so called form factor, procedure recommended for the ITTC. In this case a form factor (1+k) is evaluated in towing tank test with low Froude number in such a way that the wave making resistance is sufficiently reduced. In this way the residual force represents only the form drag.

Clearly the parcels of wave making and form drag are related, but we have obtained reasonable results assuming its independence. The form factor value was obtained experimentally, being (1+k)=1.1 and with this information we get the estimate of each parcel of the residual resistance: F_{form}=6.51N and F_{wave}=9.33N, the form and wave making resistances respectively.

Two other estimate methods would be used. The so called method of Holtrop [4 & 5] and experimental data as presented for Hughes & Cutland [6] from towing tank tests with models of similar characteristics and corrected by a curve of trends. In the case of Holtrop we get a parcel of wave making resistance of F_{wave}=11.2N. However Holtrop's method presents a total resistance (Rt) some higher than the obtained experimentally and considering that the viscous parcel estimate follows the ITTC methodology, the method seems to overestimate the parcel due to wave making. The results obtained from Hughes & Cutland [6] also presents a bigger discrepancy with a total resistance Ft=91.08N, and therefore will not be considered here for comparison.

In conclusion the parcel of residual resistance of the simulation could be compared only with the form parcel F_{form}, calculated with the ITTC methodology, using the form factor (1+k), and excluding the effect of the wave making resistance, case in which it would arrive at a total resistance in the test Ft=71.61 N, comparable to the Ft=72.54N obtained in the simulation with the mesh I for example. This is equivalent to an error of 1.23% in the total resistance, but it still has a difference of about 52% in the form drag. The figure 8 shows a comparative between the pressure distribution over the hull obtained experimentally and by the simulation. It is easy to see the at the stern the measured

average pressure is superior to the calculated results. Therefore it is expected that the result of the CFD simulation would show an overestimated form resistance.

Given the difference in the results before and after the correction of the mesh elements shape, shown in the table 3, it seems that this is the factor with most influence on the precision of the numerical model until this moment. There is also a relation between the wave making itself and the pressure distribution across the hull that is quite difficult to estimate but can be expected that a better control of the mesh will improve the simulation precision.

Some additional comments must be made with relation to the used meshes. First, observing the 3 cases studied initially (II, III and IV), we can see a gradual increase of the viscous resistance and a relatively small change of the residual resistance, in this case without the free surface, referring only to the form drag. This behavior was expected once the coarsest mesh already had a good number of elements spread on the surface, what should guarantee a good definition of the pressure distribution. On the other hand the worse refinement placed the first element more distant from the wall, and because this the wall friction got a worse estimate. This probably happens because the wall function is especially sensitive to the position of the first node.

Anyway by the presented trend of the difference between the experimental and calculated values, we would expect that with more mesh refinement the error would reduce still more. However as can be seen in case I, it did not happen. The value of the module of total resistance and the form drag in the bow increased, but not more than it was expected. But the viscous parcel had a significant reduction, opposing the observed trend. In the stern it is seen a reduction of the drag form parcel.

In a general way, inflection points at the trend curves are not expected and this happened both at the bow and stern of the hull. See figure 4.

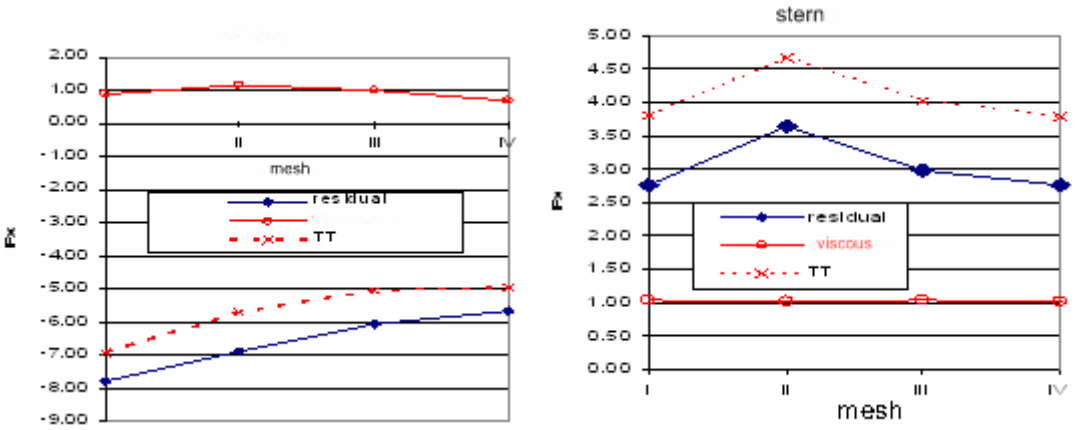

Figure 4. Chart with the force values at the x direction from the grid convergence test. Bow data at left, and stern data at the rigth

Apparently in the region of the bow, in cases II, III and IV, the high skewness of the elements and the distance of the first node from the wall had made difficult the correct capture of the behavior of the boundary layer. It was a localized error and due to strong bending of the wall in that region. In the stern the effect of the mesh refinement was more felt in the drag form that had an unexpected variation. As meshes II, III and IV did not present great problems at the stern region, it was not possible to understand this behavior. The calculated values of the force are shown in table 3.

Table 3: Numerical results at each hull's section.. Fxp: pressure force at x direction; Fxv: Viscous force at x direction; Fxt: total force. Force values in Newton (N).

	Bow			mid-section			stern			Sum		
	Fxp	Fxv	Fxt	Fxp	Fxv	Fxt	Fxp	Fxv	Fxt	Fxv TT	Fxp TT	**Fx TT**
I	7.80	-0.89	6.91	-14.92	-60.73	-75.65	-2.76	-1.04	-3.80	-62.66	-9.88	**-72.54**
II	6.88	-1.18	5.70	-14.94	-60.34	-75.27	-3.64	-1.02	-4.66	-62.54	-11.70	**-74.23**
III	6.05	-1.01	5.04	-15.64	-58.88	-74.52	-2.98	-1.05	-4.03	-60.94	-12.57	**-73.51**
IV	5.66	-0.70	4.97	-16.06	-55.76	-71.83	-2.76	-1.03	-3.78	-57.49	-13.16	**-70.64**

To achieve the validation of the model, when the mesh refinement is increased, the numerical error should decrease asymptotically to zero. Of course we could not use a mesh so refined in order to achieve a zero numerical error but using three or more simulations with different grid refinement it is possible to estimate the exact answer and from this,

the uncertainty of the simulation result. Due to divergence of the results from the mesh refinement in this case it is not possible to get the validation of the model, and the estimate of the numerical uncertainty of the solution.

3.2. Flow

The figure 5a below gives an overview of the evolution of the wake around of the hull. In a general way it can be seen that it has a small thickness until the middle of the hull, and goes growing quickly in the region of the stern caused by the surface bending. Observing the wake in the region of the propeller entrance plane it is possible to see the typical asymmetry of the speed profile in this region. The "upper side" of the propeller operates in a region of reduced incident flow velocity.

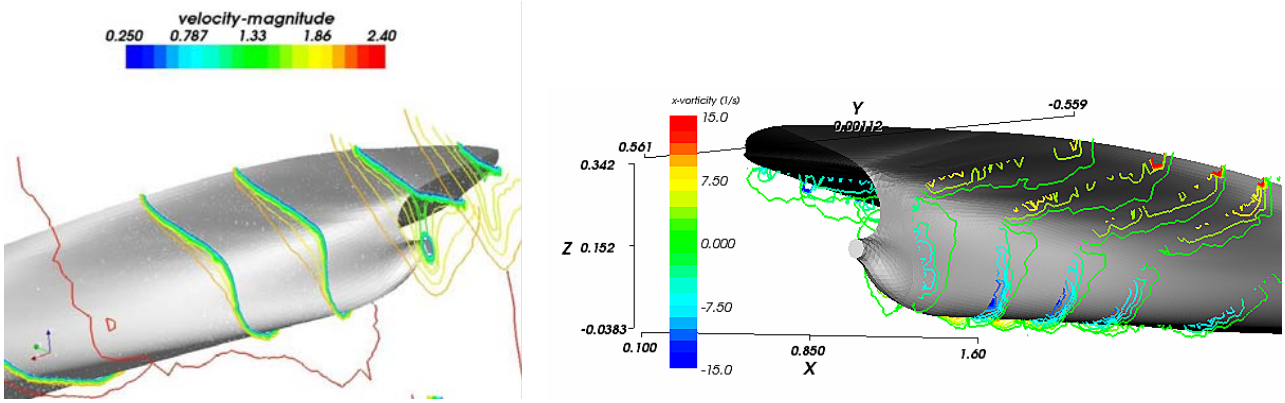

Figure 5: at left (a) the velocity magnitude contours; (b) at the right shows the radial vorticity contours;

In the figure 6 below we see a comparison between the experimental and the calculated values of the wake axial velocity profile in three different sections. A difference in the geometry of the boundary layer can be clearly seen in the concave region of the hull. Despite this the mean distance of the iso-velocity lines to the wall is compatible between the two results. Still so a bigger concentration of the lines is noticed next the wall in the result of the calculation what demonstrates a faster increase of the velocity profile than is expected. As the total thickness is close to the experimental one, the modeling in the internal region of the boundary layer seems to be the problem what means that the accuracy of the wall functions in this case is deficient.

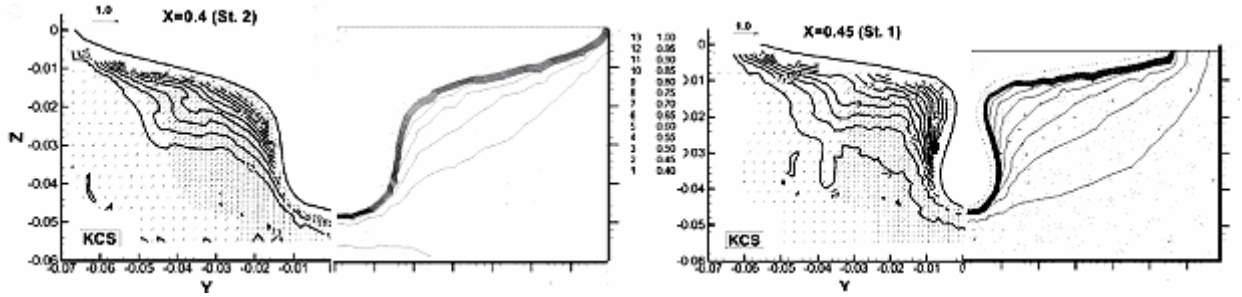

Figure 6: Comparison between the experimental data and the numerical data at two different cross sections along the hull. At the left of each figure is the experimental data obtained from [10] and at the right the calculated;

In the figure 7 it is shown one more detail of the profile obtained experimentally with the calculated one. Despite the iso-velocity lines not being in the same position, there is a good agreement between them, except in the superior position (90°) where the calculated speed is significantly higher (V/Ve = 0.45 in the experimental case and the 0.65-0.7 in the calculated one).

Also it is well known the phenomenon of axial vortices generation in the stern at this type of hulls. The vortex creation is essentially a three-dimensional phenomenon and has influence on the velocity of the wake that arrives at the propeller plane, once the vortex passes through the central section of the ship. Such effect can be seen in figure 5b. The axial vorticity contours shows an increase of the velocity in the lower region of the hull, going up in the direction of the propeller plane. Looking at the pressure distribution and the streamlines in this region, such as expected, the rotation direction indicates that the flow comes from the region of low pressure for the high-pressure, indicating that the detachment occurs exactly in the region of adverse pressure gradient.

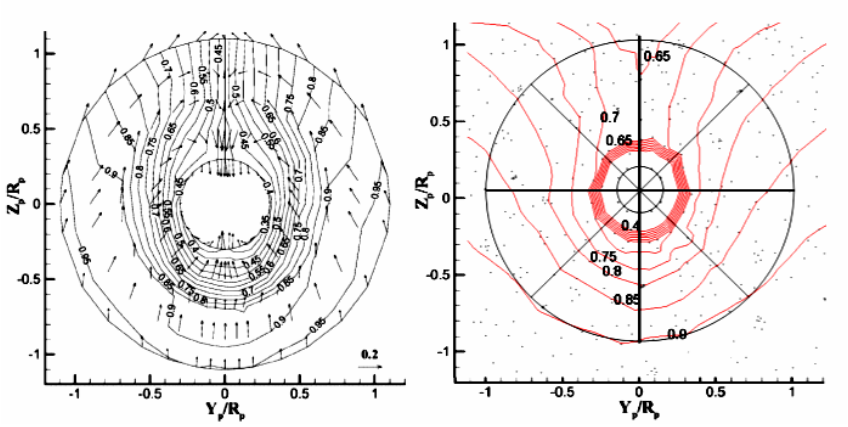

Figure 7: Comparative of the propeller plane axial velocity contours. At the left the experimental chart obtained from [10] and at right the evaluated. One important detail is that at the left the inner and outer circle represents 30% and 110% of the propeller diameter and at the right represents the shaft and the propeller diameters.

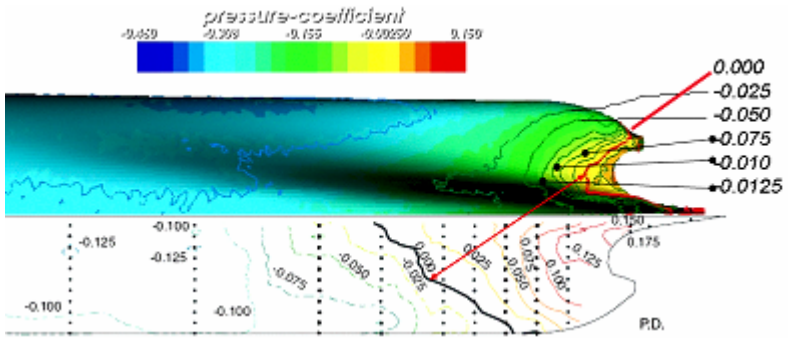

Figure 8. The pressure coefficient contours from de simulation (upper side) and from the experiment;

The figure 8 above shows a comparison between the calculated and measured static pressures on the hull, at the stern position. The zero *Cp* line was highlighted to best show the differences. The simulation concentrate de high pressure region on a smaller area close to the rear of the stern. The measured pressure field indicates a better pressure distribution in a bigger area. We suspect that the difference it is caused by the absence of the free surface interaction, and an improvement of the calculated result could not be obtained without taking into account the effects of the free surface.

4. Conclusion

The method is qualitatively in good agreement with the experimental data. The predicted total resistance is smaller than the measured and the relative error is greater than the benchmarks from other similar works. From the numerical data it can be observed some differences at the boundary layer velocity profile which leads to a difference in the obtained wall friction and turbulence generation and dissipation.

Based on the pressure distribution on the hull at the stern, where the wave generation effects are greater, the major source of difference it is probably the absence of the free surface. But the grid convergence study shows also that the bad quality of the volumes especially close to the hull surface strongly affect the accuracy of the evaluated resistance.

The model can be improved with the help of a multi-block approach using structured grids at the less bended region of the surface and restricting the use of very refined unstructured meshes only at the most geometrically complex parts of the hull.

The wall functions have shown a worse performance at the stern where the flow is more curvilinear and there is a strong adverse pressure gradient. But the relative few time expended at the grid generation and simulations and the relative good agreement obtained show that with some more improvements the method could be used at an engineering level as a help to the study of the main characteristics of different geometries, and their optimization.

5. References

[1] Carlon, J. S.; Marine Propellers and Propulsion; Butterworth-Heinemann; England; 1994;
[2] Hackett, J.P.; Brewer, W.H.; Manufacturing Tolerante Effects on Ship Rudder Performance; Technology Review Journal; 2004;
[3] Hellsten, A; Laine, S; Extensión of the k-w turbulence model for flows over rouge walls; AIAA AFM Conference papers; 1997;
[4] Holtrop, J.; An approximate Power Prediction Method; International Shipbuilding Progress; Vol. 29; July; 1982;
[5] Holtrop, J.;Mennen G. G. J.; A statistical re-analysis of resistance and propulsion data; International Shipbuilding Progress; Vol. 31; November; 1984;
[6] Hughes, G.; Cutland, R.S.; Viscous and Wave Components of ship model resistance; National Physical Laboratory; England; Vol. I & II; 1973;
[7] ITTC (International Towing Tank Comitee) Recommended Procedure 7.5-02-02-01;Testing and Extrapolation Methods-Resistance Test; 2002;
[8] ITTC Recommended Procedure 7.5-02-03-01.4; Performance Prediction Method; 1978;
[9] Kalitzin, G; Medic, G; Iaccarino, G; Durban, P; Near wall behavior of RANS turbulence models and implications for wall functions; Journal of Computacional Physics; article in press (2005);
[10] Kim, J.W; Van S.H; Kim, D.H; Measurement of flows around modern comercial slip models; Experiments in Fluids; vol. 31; pp 567-578; 2001;
[11] Kral; L.D; Recent experience with diferente turbulence models applied to the calculation of flor over aricraft components; Progress in Aerospace Sciences; Vol. 34; pp 481-541; 1998;
[12] MARNET CFD Final Report and Review of the State of the Art in the Application of CFD on the Maritime and Offshore Industries; 2003;
[13] Reddy, K.R.; Toffoletto, R.; Jones, K.W.; Numerical Simulation of Ship Airwake; Computer & Fluids; vol. 29; 2000;
[14] Simonsen, C. D; Rudder, Propeller and Hull Interaction by RANS; Technical University of Denmark; PhD Thesis; 2000;
[15] Simonsen, C. D.; Stern, F.; Flow pattern around an appended tanker hull form in simple maneuvering conditions; Computers & Fluids; vol. 34; 2005
[16] Simonsen, C. D.; Stern, F.; Verification and validation of RANS maneuvering simulation of Esso Osaka: effects of drift and rudder angle on forces and moments; Computer & Fluids; vol. 32; 2005
[17] Sing-Kwan, L.; Ah Kuan, S.; Integrated Simulation System for Propeller Excitation Problems – ABS Technical Capabilities; 26th Annual Journal of Society of Naval Architects & Marine Engineers; 2002/03; Singapure;
[18] Stern, F.; Wilson, R. V.; Coleman, Hugh W.; Paterson, E. G.; Comprehensive approach to verification and validation of CFD simulations – Part 1: Methodology and Procedures; Journal of Fluids Engineering; Vol. 123; December; 2001;
[19] Stern, F.; Wilson, R. V.; Coleman, Hugh W.; Paterson, E. G.; Comprehensive approach to verification and validation of CFD simulations – Part 2: Application for Rans simulation of a Cargo/Container Ship; Journal of Fluids Engineering; Vol. 123; December; 2001;
[20] Tahara, Y.; Stern, F.; A Large-Domain Approach for Calculationg Ship Boundary Layers and Wakes and Wave Fields for Nonzero Fraude Numbers; Journal of Computacional Physics; Vol 127; 1996
[21] Wilcox, D. C; Turbulence Modeling for CFD; DCW Industries; 2nd edition; 2000;

5. Responsibility notice

The authors Carlos J. Rocha O. Castro and Fabio Saltara are the only responsible for the printed material included in this paper.